PREMIXED FLAME INHIBITION BY MANGANESE AND TIN COMPOUNDS*

Gregory T. Linteris†, Vadim Knyazev, and Valeri Babushok
National Institute of Standards and Technology

INTRODUCTION

The production ban on the effective, bromine-based fire suppressants due to their ozone depletion potential has motivated the search for alternative compounds. Iron has been shown to be up to two orders of magnitude more effective than Br as a flame inhibitor; however, it loses its effectiveness due to condensation of the active species to particles. Consequently, it is of interest to determine if other metals cause similar strong flame inhibition while not suffering from the loss of effectiveness. Since manganese and tin have higher vapor pressures than iron, Table 1, these compounds are potential additives for effective fire suppression. The present work seeks to determine the gas-phase flame inhibition properties of tin and manganese through experiments and modeling of their reduction in the premixed burning velocity of methane – air flames.

Table 1 - Saturated vapor pressures for some Fe-, Mn-, and Sn-containing species.

	Partial Pressure, atm.					
T K	**Fe**	**Mn**	**Sn**	**FeO**	**MnO**	**SnO**
1500	2.E-6	1.04E-3	1.14E-5	1.53E-10	3.75E-11	4.7E-3
2000	3.69E-4	0.126	4.34E-3	2.3E-6	1.3E-6	0.639
2500	3.09E-2		0.153	5.7E-4	4.26E-4	

It is well known that metals can catalyze the recombination of radicals in the post combustion region of hydrogen – air flames [1-4]. Bulewicz and Padley demonstrated that metallic compounds of Cr, Mn, Sn, U, Mg, and Ba accelerate hydrogen atom recombination at ppm‡ levels. Nonetheless, careful studies of flame inhibition, with the goal of assessing the metals' effects on the overall reaction rate, are limited. Tin compounds are widely used in semiconductor industry. They are fire retardant additives for polymers, and are used to reduce smoke and CO formation. [5, 6]. The mechanism of flame inhibition has been attributed to both condensed phase char promotion and gas-phase flame inhibition [6, 7]. Lask and Wagner [8] found $SnCl_4$ to be about 1/34 as effective as $Fe(CO)_5$ at reducing the burning velocity of premixed n-hexane–air flames by 30 %, and Miller et al. [9] found it to be about 2/3 as effective as $Fe(CO)_5$ at reducing the flame speed of hydrogen-air flames by 80 %. Miller [10] measured the amount of inhibitor required to lift-off a premixed, $CH_4/O_2/N_2$ flat flame at low pressure, and found that $Sn(CH_3)_4$ (TMT) and $SnCl_4$ required a mole fraction of

* Official contribution of NIST, not subject to copyright in the United States.

† Corresponding author

‡ all references to ppm in the present paper are on a volume basis, and refer to μL/L.

1.7 % and 1.1 %, whereas $Fe(CO)_5$ and Br_2 required 0.23 % and 2.3 %. Morrison and Scheller [11] investigated the effect of 20 flame inhibitors on the ignition of hydrocarbon mixtures by hot wires, and found that $SnCl_4$ was the most effective inhibitor for increasing the ignition temperature; whereas CrO_2Cl_2 and $Fe(CO)_5$, powerful flame inhibitors, had no effect on the ignition temperature. As a result of these studies, tin tetrachloride $SnCl_4$ was recommended as compound deserving further study [12].

Manganese compounds have also been studied. Vanpee and Shirodkar [13] investigated the effect of many metal chlorides and metal acetates and acetylacetonates on the limiting oxygen index at extinction in a partially premixed counterflow pool burner of ethanol and air. In their experiment, the inhibitor was dissolved into ethanol, which was aspirated into the air stream. They found manganese acetylacetonate to be more effective than acetylacetonates of iron or chromium. Westblom et al. [14] analyzed the effect of trace amounts of methylcyclopentadienylmanganese tricarbonyl ($C_9H_7MnO_3$, MMT) on the flame structure of a premixed propane - air flame at 40 torr, but found no measurable effect. They did, however, suggest a kinetic model for the influence MMT on those flames. In a review article, Howard and Kausch [5] reported that manganese-containing compounds are among the most effective soot-reducing fuel additives. Finally, MMT is a known antiknock agent in gasoline [15]. In the report of NMERI (Albuquerque, NM) manganese compounds were suggested as the agents for further consideration and studies of fire suppression performance [16].

EXPERIMENT

The laminar flame speed S_L provides a measure of an agent's reduction of the global reaction rate. The experimental arrangement, described in detail previously [17-20], has been modified to accommodate new evaporators for TMT and MMT. A Mache-Hebra nozzle burner (1.0 cm ± 0.05 cm diameter) produces a premixed Bunsen-type flame about 1.3 cm tall with a straight sided schlieren image that is captured by a video frame-grabber board in a PC. Digital mass flow controllers hold the oxygen mole fraction in the oxidizer stream $X_{O2,ox}$, the equivalence ratio ϕ, and the flame height constant while maintaining the inlet mole fraction of the inhibitor (X_{in}) at the desired value. The average burning velocity is determined from the reactant flows and the schlieren image using the total area method. The fuel gas is methane (Matheson* UHP, 99.9 %), and the oxidizer stream consists of nitrogen (boil-off from liquid N_2) and oxygen (MG Industries, H_2O < 50 ppm, and total hydrocarbons < 5 ppm). The inhibitors used are $Fe(CO)_5$ (Aldrich), TMT (Alfa Aesar), MMT (Alfa Aesar), CF_3Br (Great Lakes), N_2 (boil-off), and CO_2 (Airgas). The $Fe(CO)_5$ is added to the carrier gas using a two-stage saturator in an ice bath, described previously [20]. Nitrogen is the carrier gas for all agents. The TMT was added using an identical two-stage saturator, with >50 cm^3 of TMT in each stage. The water bath was maintained at (0 ± 0.2) °C with a maximum

* Certain commercial equipment, instruments, or materials are identified in this paper to adequately specify the procedure. Such identification does not imply recommendation or endorsement by the National Institute of Standards and Technology, nor does it imply that the materials or equipment are necessarily the best available for the intended use.

carrier gas flow 0.40 L / min. For the MMT, the saturator had three stages, each a 20 cm long, 2.36 cm I.D. stainless steel tube, and the entire apparatus was submerged in a controlled temperature bath (Neslab). The bath temperature was typically (79.2 ± 0.1) °C, and the carrier gas flow for this saturator was always <0.5 L / min. The mole fraction of the organometallic inhibitors in the air stream was calculated based on the measured air flow, measured carrier gas flow, and vapor pressure of the agent at the bath temperature, assuming saturated carrier gas. The parameters in the Antoine equation $\log_{10}(P)=A-B/(T+C)$, T in °C, P in bar, are (A,B,C): (6.77273, 4.0932, 7.2283), (1258.22, 1286.16, 1882), and (211.587, 235.846, 200) for $Fe(CO)_5$ [21], TMT [22], and MMT[23]. Since the vapor pressure of MMT is much lower than that of the other agents, any tests with MMT used heaters and temperature controllers to maintain the transfer lines and inlet gases at (80 ± 3) °C and the burner tube at (80 ± 1) °C. Tests were performed for a range of stoichiometry ϕ and oxygen mole fraction in the oxidizer stream $X_{O_2,ox}$. The agent mole fraction is calculated relative to the total reactant flow.

Determination of the uncertainties in the experimental data using the present apparatus has been described in detail previously [20]. For the present data, the uncertainty (expanded uncertainties with a coverage factor of 2) in the normalized burning velocity are less than ± 5 % for all cases. The uncertainty in the equivalence ratio is 1.4 %. Neglecting the uncertainties (unspecified) in the vapor pressure correlation for $Fe(CO)_5$, TMT, and MMT, uncertainties in the bath temperature, ambient pressure and carrier gas flow rate yield an inhibitor mole fraction uncertainty of 6.5 %.

KINETIC MECHANISMS AND NUMERICAL MODELING

There is little data on the chemical kinetics of tin compounds at flame temperatures. Kinetic studies of tin have been conducted for chemical vapor deposition. Studies in hydrogen-oxygen-nitrogen flames by Bulewicz and Padley [24] indicate that tin is present as Sn, SnO, and SnOH, with SnO the overwhelmingly predominant species. Recent spectroscopic data also indicate that tin is presents in flames as SnO, SnOH, and Sn [25], with SnO and SnOH accounting for >97 % and <3 % of the tin, and Sn accounting for very little.

The present kinetic model for tin flame inhibition contains reactions of Sn, SnO_2, SnO, SnH and SnOH. The reaction set is based on the consideration of possible reactions of tin-containing species with the radical pool and the main species of methane combustion. The model [26] consists of 37 reactions with tin-containing species, and includes TMT decomposition to Sn atom. Enthalpies of formation for the tin-containing species are presented in

Table 2.

Table 2 - Enthalpy of formation for some manganese- and tin-containing species (298K).

Species	Enthalpy of Formation kJ/mol	Ref.	Species	Enthalpy of Formation kJ/mol	Ref.
Mn	283.6	[27]	Sn	301.2	[27]
MnO	161.7	[27]	SnO	21.91	[27]
MnO_2	23.01	[27]	SnO_2	11.69	[27]
MnOH	17.32	[27]	SnOH	-15.06	*
$Mn(OH)_2$	-373.2	*	SnH	268.2	*
MnOOH	-116.3	*	$Sn(CH_3)_4$	-17.70	[28]
MnH	197.9	[27]	Sn_2	425.4	[27]
MMT	-439.3	[14]			

* Estimation.

The kinetic mechanism for studying the influence of manganese additives in premixed methane-air flames is also presented in reference [26]. The list of possible Mn-containing species participating in inhibition reactions includes Mn, MnH, MnO, MnOOH, MnHOH, MnOH, MnO, MnO_2 and $Mn(OH)_2$. All of these except MnH and MnHOH were considered in a mechanism of Smith et al. [29]. The role of MnOH and MnO in radical recombination was discussed by Bulewitz and Padley [1], and the species MnO and Mn were recently measured in a low pressure propane flame doped by MMT [14]. Hildenbrand and Lau [30] used mass spectrometry to identify the species MnO_2, MnOH, $Mn(OH)_2$. We included the species MnH in the model since equilibrium calculations showed it to be a significant compound of manganese in flames.

Table 2 contains enthalpies of formation for manganese-containing species considered in kinetic model.

For the manganese inhibition reaction set, we generated a comprehensive list of approximately 160 reactions of Mn-containing species with radical pool species and the main species of methane combustion. This list was reduced to 61 reactions based on thermochemical considerations and preliminary calculations. This reaction set does not contain a decomposition route for the Mn-containing parent molecule. For MMT decomposition, we adopt the description of Smith [29], and use their rates for other Mn-species reactions where possible. Rate constants for the remaining reactions were estimated by analogy with reactions for iron containing species [31]. The main assumptions are the formation of MnO_2 through the reaction of Mn atom with oxygen molecule and formation of $Mn(OH)_2$ in reactions similar to reactions of iron-containing species.

Kinetic models for highly effective flame inhibitors can be considered to consist of two sub-models. The first sub-model includes reactions for agent decomposition and formation of the active inhibiting species, and the second includes the inhibition reactions. In previous work, it has been shown that for the phosphorus-containing compound DMMP and for ferrocene, the decomposition reactions have a small influence on the predicted inhibitor efficiency as long as the overall activation energy of

decomposition is less than (250 to 335) kJ/mol. In the present work, this was also found to be true for TMT and MMT decomposition.

The laboratory flames inhibited by TMT and MMT were numerically modeled as one-dimensional freely-propagating flames. Solutions were obtained using the Sandia flame code *Premix* [32], and the *Chemkin* [33] and transport property [34] subroutines. The kinetic mechanism for methane combustion was from GRIMech 3.0 [35], with the nitrogen chemistry removed; this sub-mechanism contains 36 species and 219 reactions. It should be emphasized that the reaction mechanisms used for the present calculations should be considered only as a starting point. Numerous changes to both the rates and the reactions incorporated may be made once a variety of experimental and theoretical data are available for testing the mechanism.

RESULTS

OBSERVATIONS

The appearance of the flames with added organometallic inhibitors is shown in Figure 1. Flames with iron are bright orange, tin are bright pale blue, and manganese, yellow-green. The intensity of all flames increases with increasing inhibitor mole fraction. As the loading of metallic inhibitor increases, there becomes visible a luminous outer shroud as seen clearly in the last two images on the right in Figure 1. We believe these are regions of high particle concentration from inhibitor condensation, leading to broad-band black body radiation, visible here in the orange part of the spectrum.

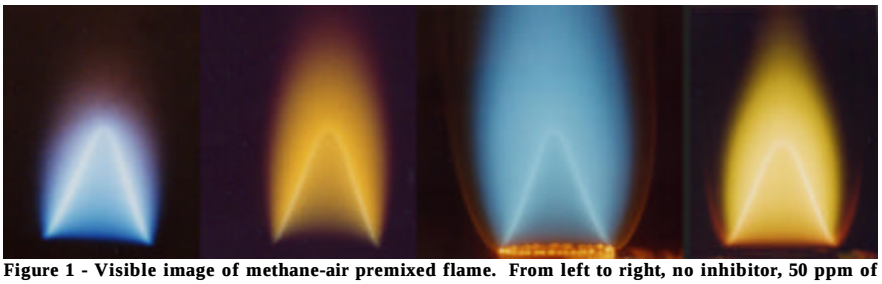

Figure 1 - Visible image of methane-air premixed flame. From left to right, no inhibitor, 50 ppm of $Fe(CO)_5$, 4000 ppm of TMT, and 400 ppm of MMT.

INHIBITION BY TETRAMETHYL TIN

Figure 2 shows the relative burning velocity reduction with addition of TMT to methane-air flames ($X_{O_2,ox}$ =0.21) for values of ϕ of 0.9, 1.0, and 1.2. The dotted lines are

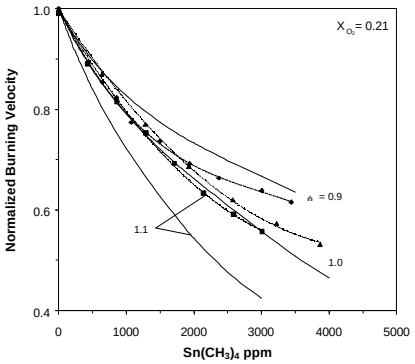

Figure 2 – Normalized burning velocity of premixed $CH_4/O_2/N_2$ flames inhibited by TMT with $X_{O2,ox}$=0.21 and ϕ=0.9, 1.0, and 1.1 (dotted lines: curve fits to data; solid lines: numerical predictions).

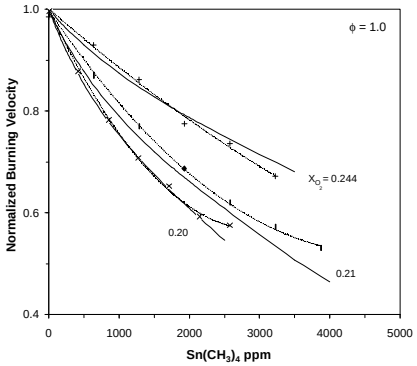

Figure 3 – Normalized burning velocity of premixed $CH_4/O_2/N_2$ flames inhibited by TMT, with ϕ=1.0 and $X_{O2,ox}$=0.20. 0.21, and 0.244 (dotted lines: curve fits to the data; solid lines: numerical predictions).

curve fits to the experimental data, and the solid lines are the results of the numerical calculations described above. Data are plotted as normalized burning velocity, which is the burning velocity of the inhibited flame divided by the value for the same flame in the absence of inhibitor. The calculated and experimental burning velocities, along with the calculated adiabatic flame temperatures of the uninhibited flames used for the normalizations are shown in Table 3. (Note that the calculations are for 1-D planar flames, while the experiments determine the average flame speed of Bunsen-type flames.) The experimental results in Figure 2 show that for stoichiometric flames, 3000 ppm of TMT reduces that flame speed by about 41 %, which is about a factor of two better than CF_3Br. The data also show that, unlike that case for $Fe(CO)_5$, the richer flames are inhibited more strongly by TMT than the leaner flames. The numerical model predicts the amount of inhibition well for stoichiometric flames; however, for lean flames the inhibition is underpredicted, while for rich flames, it is overpredicted. Figure 3 shows the measured and calculated flame speeds for TMT in stoichiometric flames with values of $X_{O_2,ox}$ equal to 0.20, 0.21, and 0.244. Here, the model predictions of the burning velocities are excellent. Nonetheless, for the slower, cooler flames of either figure (e.g. ϕ=0.9 or 1.0 with $X_{O_2,ox}$ = 0.20 or 0.21), the TMT starts to lose its effectiveness above a certain value, as did $Fe(CO)_5$ (the cause of which was shown to be condensation of the iron-containing intermediates [19]).

Table 3 - Uninhibited laminar burning velocities S_L and adiabatic flame temperature T_{AFT} from 1-D planar numerical calculations and from average burning velocity in Bunsen-type flame experiment.

ϕ	$X_{O_2,ox}$	T_{in} K	T_{AFT} K	$S_{L,calc.}$ cm/s	$S_{L,exp}$ cm/s
TMT					
0.9	0.21	298	2159	35.3	33.9 ± 1.3
1.0	"	"	2235	39.6	38.0 ± 2.3
1.1	"	"	2193	39.8	38.0 ± 1.5
1.0	0.20	"	2185	34.7	33.6 ± 1.4
"	0.244	"	2377	57.0	58.0 ± 3.4
MMT					
0.9	0.21	353	2177	48.0	47.2 ± 1.5
1.0	"	"	2264	53.2	52.9 ± 2.9
1.1	"	"	2251	53.6	52.8 ± 2.0
1.0	0.19	"	2167	41.3	39.9 ± 1.6
"	0.2	"	2220	47.4	45.5 ± 1.7
"	0.244	"	2396	74.3	74.7 ± 4.1

INHIBITION BY MMT

The premixed flames inhibited by manganese are slightly preheated (T_{in} = 80 °C), and the values of the calculated and experimental uninhibited burning velocities, and the adiabatic flame temperatures are shown in Table 3. The normalized burning velocity of MMT-inhibited flames with variation in ϕ and $X_{O_2,ox}$ are shown in Figure 4 and Figure 5. MMT is seen to be about 15 times more efficient at flame inhibition than TMT; however, it too starts to lose its effectiveness for flame speed reductions near 50 %. The model predicts the burning velocity reduction quite well, although it underpredicts the inhibition somewhat in all cases, and the discrepancy gets larger as the value of $X_{O_2,ox}$ (and the flame temperature) increases.

Figure 6 compares the performance of $Fe(CO)_5$, MMT, TMT, $SnCl_4$, and CF_3Br. The data for $SnCl_4$ in n-hexane – air flames [8] show it to be as effective as TMT is in these methane – air flames. As the figure also shows, $Fe(CO)_5$ is significantly more effective than any of the other agents, and all appear to have greatly reduced effectiveness at burning velocity reductions of about 50 %.

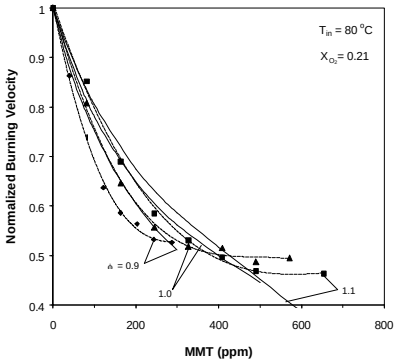

Figure 4 - Normalized burning velocity of premixed $CH_4/O_2/N_2$ flames inhibited by MMT with $X_{O2,ox}$=0.21 and ϕ=0.9, 1.0, and 1.1 (dotted lines: curve fits to data; solid lines: numerical predictions).

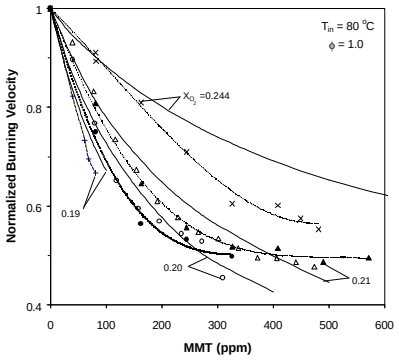

Figure 5 - Normalized burning velocity of premixed $CH_4/O_2/N_2$ flames inhibited by MMT, with ϕ=1.0 and $X_{O2,ox}$=0.19, 0.20. 0.21, and 0.244 (dotted lines: curve fits to the data; solid lines: numerical predictions).

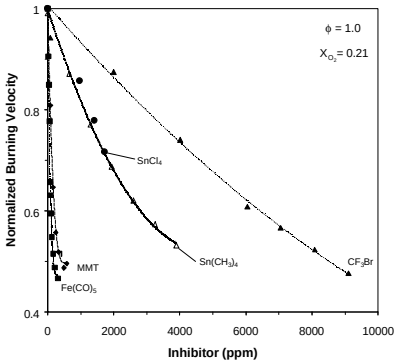

Figure 6 - Normalized burning velocity of premixed $CH_4/O_2/N_2$ flames inhibited by CF_3Br, TMT, $SnCl_4$ [8], MMT, and $Fe(CO)_5$ (T_{in} = 80°C for all data except TMT and $SnCl_4$ (lines are curve fits to data).

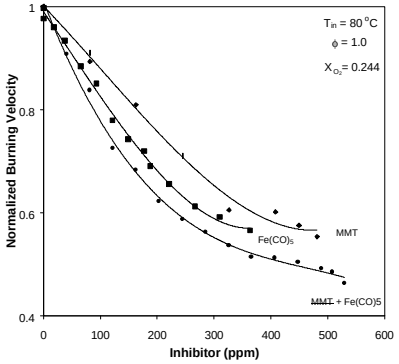

Figure 7 - Normalized burning velocity of premixed $CH_4/O_2/N_2$ flames inhibited by pure MMT and $Fe(CO)_5$, and by a blend of the two (lines are curve fits to the data).

One approach for overcoming the loss of effectiveness is to add non-condensing amounts of several inhibitors. To test this approach in premixed flames, we performed

tests with a blend of MMT and $Fe(CO)_5$, added at a molar ratio of 2:1, respectively. For the flame of this test, T_{in} = 80 °C, ϕ=1.0, and $X_{O_2,ox}$=0.244; data for pure MMT or $Fe(CO)_5$ and the combination are shown in Figure 7 (the data for the combination are plotted as a function of the mole fraction of the more abundant agent, MMT). As the figure shows, adding 0.5 moles of $Fe(CO)_5$ for each mole of MMT added does provide additional flame speed reduction over that from MMT alone.

BLENDS OF MMT AND $FE(CO)_5$

The behavior of the blends of agents can be investigated by comparing the actual amount of flame speed reduction for the blend to the sum of the inhibition which would result from each agent individually. This approach is illustrated schematically in Figure 8. We adopt the inhibition index $\Phi(X_{in})$ of Fristrom and Sawyer [36], where $\Phi(X_{in})=\{\{(V_o-V(X_{in}))/V_o\}\{X_{O_2,ox}/X_{in}\}$ (and using the oxygen mole fraction in the oxidizer). The index $\Phi(X_{in})$ is seen to be the magnitude of the average slope of the normalized burning velocity curve (times $X_{O_2,ox}$) evaluated at the mole fraction of interest X_{in}. For a given blend, we can evaluate the amount of normalized burning velocity *reduction* that would have been caused by each individual component of the blend, say components *a* and *b*. The predicted inhibition index is just a linear combination of the reduction from each component, or $X_a \cdot \Phi_{a+b}(X_a, X_b)|_{pred} = X_a \cdot \Phi_a(X_a)+X_a \cdot \Phi_b(X_b)$, in which *a* is the major component of the blend, (and we have selected it for defining $\Phi_{a+b}(X_a, X_b)$). The actual inhibition index $\Phi_{a+b}(X_a, X_b)|_{actual}$ is evaluated from the normalized flame speed of the blend (using X_a in its definition). The ratio of $X_a \cdot \Phi_{a+b}(X_a, X_b)|_{actual}$ to $X_a \cdot \Phi_a(X_a)+X_a \cdot \Phi_b(X_b)$ provides a reasonable indicator of the performance of the blend relative to the individual components.

As Figure 9 shows, a blend of CO_2 and N_2 (in the molar ratio of 1:2) provides a performance index of nearly 1.0 for N_2 added up to 12 % (i.e. containing 6 % CO_2). (The percent of the N_2/CO_2 mix in Figure 9 is divided by twenty to allow placement on the same scale.) The blends of CF_3Br and ferrocene (Fec) also perform approximately like the linear combination of the performance of each (a performance ratio near 1.0 in Figure 9. Note that in the Fec/CF_3Br blend, the maximum amount of Fec is 23 ppm and 66 ppm for the curves marked 0.36 % and 1.33 % Fec, respectively. For similarly low levels of metallic inhibitors, the blend of MMT and $Fe(CO)_5$ also behaves like sum of the individual contributions; however, as the amount of inhibitor increases, the performance of the blend is much less. This is likely due to condensation of mixed oxide species [37], showing that this approach may have limitations.

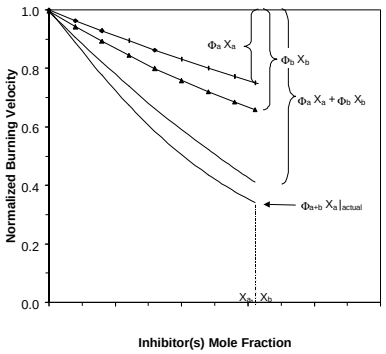

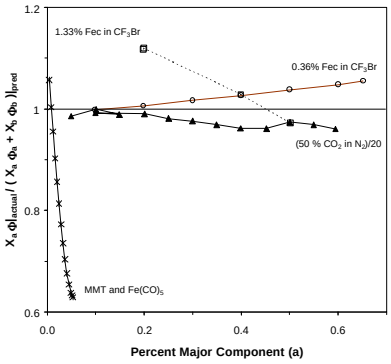

Figure 8 – Illustration of linear contribution of burning velocity reduction from each component of a two-component blend of inhibitors, together with the actual reduction from the blend.

Figure 9 - Ratio of the actual reduction in S_L from the two component mix to the predicted reduction based on linear combination of the effect from each component. The percent CO_2/N_2 has been divided by twenty to fit on the figure.

DISCUSSION

Examination of species profiles, reaction flux, and sensitivity coefficients from the numerically predicted flame allows investigation of the mechanisms of inhibition of these metallic compounds. The calculations show that TMT decomposes quickly in the flame, with 90 % consumption at 1000 K. The tin atom formed as a result of TMT decomposition quickly reacts with O_2 to form tin oxide through the reaction $Sn+O_2=SnO+O$. This reaction is fast at room temperature, as compared to the analogous reaction of iron [38]. Formation of SnO leads to the following reactions with H and HCO radicals:

$$SnO+H+M=SnOH+M$$

$$SnO+HCO=SnOH+CO$$

which, together with the radical scavenging reactions of SnOH, completes the catalytic radical recombination cycle:

$$SnOH+H=SnO+H_2$$

$$SnOH+OH=SnO+H_2O$$

$$SnOH+CH_3=SnO+CH_4.$$

Equilibrium calculations show that SnO is the dominant tin species in the products of a stoichiometric methane – air flame. Of the reactions of tin compounds, the burning velocity is most sensitive to the rate of the reaction SnO+H+M=SnOH+M, which has a sensitivity about four times less than the chain-branching reaction $H+O_2=OH+O$. The burning velocity is next most sensitive to the tin reactions: $Sn+CO_2=SnO+CO$, $SnO+HCO=SnOH+CO$, $SnOH+H=SNO+H_2$, and $SnOH+OH=SNO+H_2O$, for which the sensitivity is about forty times less than the chain branching reaction.

As was also found for DMMP and ferrocene, the burning velocity of flames inhibited by TMT is not sensitive to the rate of the decomposition reaction. Numerical tests showed that changes in the overall activation energy of TMT decomposition in the range 170 kJ/mol to 335 kJ/mol yield little effect on the burning velocity with up to 2000 ppm of TMT. Hence, the inhibition effectiveness of tin compounds is likely to be independent of the parent molecule, as long as rapid decomposition occurs. The rate selected for the pre-exponential factor of the association reaction SnO+H+M=SnOH+M has a significant effect on the predicted burning velocity (in the present mechanism, $A=5.5 \times 10^{17}$ $cm^6 \cdot s^2 \cdot mol^{-2}$)

Note that similar to what was found for $CO - N_2O$ flames inhibited by $Fe(CO)_5$, the reactions $SnO+CO=Sn+CO_2$ and $Sn+O_2=SnO+O$ can promote the CO consumption and decrease the inhibition effect of tin. Changes in these rates can also affect the inhibition efficiency of tin, although the mechanism is dominated by the rate of reaction SnO+H+M=SnOH+M.

Analysis of the numerical results for inhibition by MMT shows that its behavior in this premixed methane-air flame is similar to that $Fe(CO)_5$, with the catalytic radical recombination cycle consisting of:

$$MnO + H_2O = Mn(OH)_2$$

$$Mn(OH)_2 + H = MnOH + H_2O$$

$$MnOH + OH \text{ (or } H) = MnO + H_2O \text{ (or } H_2).$$

Although flame equilibrium calculations show that the species MnH is present at relatively large concentrations, the contribution of reactions of this species to the inhibition effect is relatively small. Sensitivity analysis demonstrates that burning velocity is most sensitive to the reactions $Mn(OH)_2+H=MnOH+H_2O$, $Mn+O_2(+M)=MnO_2(+M)$, $MnOH+O+M=MnOOH+M$, $MnOOH+H=MnO+H_2O$, $MnOH+OH=MnO+H_2O$, $MnO+H=Mn+OH$, and $MnO+H_2=Mn+H_2O$ (in decreasing order of importance), and is less sensitive to the reaction $MnO+H_2O=Mn(OH)_2$.

CONCLUSIONS

In this work we presented the first experimental measurements of influence of manganese- and tin-containing compounds (MMT, TMT) on burning velocity of methane/air flames. We have also developed kinetic models describing the inhibition mechanisms. Comparisons with $Fe(CO)_5$ and CF_3Br demonstrate that manganese and tin-containing agents are effective inhibitors. The inhibition efficiency of MMT is about a factor of two less than that of iron pentacarbonyl, and that of TMT is about twenty-six times less effective, although TMT is about twice as effective as CF_3Br. There exist conditions for which both MMT and TMT show a loss of effectiveness beyond that expected due to radical depletion, and the cause is believed to be particle formation.
Simulations of MMT- and TMT-inhibited flames show reasonable agreement with experimental data. The decomposition of the parent molecule for the tin and manganese species is found to have a small effect on the inhibition properties for the concentrations in this work. Calculations confirmed that the main species of tin compounds in the flame zone is SnO, while the concentration of SnO_2, SnOH and Sn are relatively small. The inhibition effect of TMT is determined mostly by the rate of the association reaction H+SnO+M=SnOH+M, and the catalytic recombination cycle is completed by the reactions SnOH+H=SnO+H_2 and SnOH+OH=SnO+H_2O. The manganese inhibition mechanism is the same as that for iron, namely: MnO + H_2O = $Mn(OH)_2$; $Mn(OH)_2$ + H = MnOH + H_2O, and MnOH + OH (or H) = MnO + H_2O (or H_2), and the burning velocity is most sensitive to the rate of the second of these.

We thank Tania Richie for help with the experiments, and W. Tsang, J.W. Fleming, Marc Rumminger, and G.P. Smith for helpful discussions. We also thank G.P. Smith for providing his MMT kinetic mechanism. This research was supported by the Department of Defense's Next Generation Fire Suppression Technology Program, funded by the DoD Strategic Environmental Research and Development Program under contract number W74RDV83528667, and by the Office of Biological and Physical Research, National Aeronautics and Space Administration, Washington, DC.

REFERENCES

1. Bulewicz, E. M. and Padley, P. J., "Catalytic Effect of Metal Additives on Free Radical Recombination Rates in H_2+O_2+N_2 Flames," *Proceedings of the Combustion Institute, Vol. 13,* The Combustion Institute, p. 73, 1971.
2. Bulewicz, E. M. and Padley, P. J., "Metal-Additive-Catalysed Radical-Recombination Rates in Flames," *Chem. Phys. Lett.,* **9,** 467, 1971.
3. Hastie, J. W. *High Temperature Vapors,* Academic Press, New York, 1975.
4. Jensen, D. E. and Webb, B. C., "Afterburning Predictions for Metal-Modified Propellant Motor Exhausts," *AIAA Journal,* **14,** 947, 1976.
5. Howard, J. B. and Kausch, W. J., "Soot Control by Fuel Additives," *Prog. Energy Combust. Sci.,* **6,** 263, 1980.

6. Cusack, P. A. and Killmeyer, A. J., "Inorganic Tin-Compounds as Flame, Smoke, and Carbon-Monoxide Suppressants for Synthetic-Polymers," *ACS Symp. Ser.,* **425,** 189, 1990.
7. Hornsby, P. R., Mitchell, P. A., and Cusack, P. A., "Flame Retardation and Smoke Suppression of Polychloroprene Containing Inorganic Tin-Compounds," *Polym. Degrad. Stab.,* **32,** 299, 1991.
8. Lask, G. and Wagner, H. G., "Influence of Additives on the Velocity of Laminar Flames," *Proceedings of the Combustion Institute, Vol. 8,* Williams and Wilkins Co., p. 432, 1962.
9. Miller, D. R., Evers, R. L., and Skinner, G. B., "Effects of Various Inhibitors on Hydrogen-Air Flame Speeds," *Combust. Flame,* **7,** 137, 1963.
10. Miller, D. R., "Inhibition of Low Pressure Flames," *Combust. Flame,* **13,** 210, 1969.
11. Morrison, M. E. and Scheller, K., "The Effect of Burning Velocity Inhibitors on the Ignition of Hydrocarbon-Oxygen-Nitrogen Mixtures," *Combust. Flame,* **18,** 3, 1972.
12. Pitts, W. M., Nyden, M. R., Gann, R. G., Mallard, W. G., and Tsang, W., "*Construction of an Exploratory List of Chemicals to Initiate the Search for Halon Alternatives*", National Institute of Standards and Technology, NIST Technical Note 1279, 1990.
13. Vanpee, M. and Shirodkar, P., "A Study of Flame Inhibition by Metal Compounds," *Proceedings of the Combustion Institute, Vol. 17,* The Combustion Institute, p. 787, 1979.
14. Westblom, U., Fernandezalonso, F., Mahon, C. R., Smith, G. P., Jeffries, J. B., and Crosley, D. R., "Laser-Induced Fluorescence Diagnostics of a Propane Air Flamewith a Manganese Fuel Additive," *Combust. Flame,* **99,** 261, 1994.
15. *Manganese Containing Antinock Compounds* (Nesmeyanov, A. N., Ed.), Nauka, Moskow, 1971.
16. Tapscott, R. E., Heinonen, E. W., and Brabson, G. D., "*Advanced Agent Identification and preliminary Assessment*", NMERI, University of New Mexico, NMERI 95/38/32350, 1996.
17. Linteris, G. T. and Truett, L., "Inhibition of Premixed Methane-Air Flames by Fluoromethanes," *Combust. Flame,* **105,** 15, 1996.
18. Linteris, G. T., Rumminger, M. D., Babushok, V. I., and Tsang, W., "Flame Inhibition by Ferrocene, and Blends of Inert and Catalytic Agents ," *Proceedings of the Combustion Institute, Vol. 28,* The Combustion Institute, p. 2939-2945, 2000.
19. Rumminger, M. D. and Linteris, G. T., "The Role Of Particles In Flame Inhibition By Iron Pentacarbonyl," *Combust. Flame,* **123,** 82, 2000.
20. Rumminger, M. D. and Linteris, G. T., "Inhibition of premixed carbon monoxide-hydrogen-oxygen-nitrogen flames by iron pentacarbonyl," *Combust. Flame,* **120,** 451, 2000.
21. Gilbert, A. G. and Sulzmann, K. G. P., "The Vapor Pressure of Iron Pentacarbonyl," *J. Electrochem. Soc.,* **121,** 832, 1974.
22. Stull, D. R., "Vapor Pressure of Pure Substances Organic Compounds," *Ind. Eng.*

Chem., **39,** 517, 1947.
23. Hollrah, D., Ethyl Corp., Personal Communication, Jan. 2001.
24. Bulewicz, E. M. and Padley, P. J., "Photometric Observations on the Behaviour of Tin in Premixed H_2-O_2-N_2 Flames," *Transactions Faraday Society*, **67,** 2337, 1971.
25. Goodings, J. M. and Chen, Q.-F., "Chemical Kinetics and Thermodynamics of Tin Ionization in H_2-O_2-N_2 Flames and the Proton Affinity of SnO," *Can. J. Chem.*, **76,** 1437, 1998.
26. Linteris, G. T., Knyazev, K., and Babushok, V., "Methane-Air Premixed Flame Inhibition by Manganese and Tin Compounds," *Combust. Flame*, (in preparation), 2001.
27. Gurvich, L. V., Iorish, V. S., Chekhovskoi, D. V., Ivanisov, A. D., Proskurnev, A. Yu., Yungman, V. S., Medvedev, V. A., Veits, I. V., and Bergman, G. A. *IVTHANTHERMO - Database on Thermodynamic Properties of Individual Substances*, Institute of High Temperatures, Moscow, 1993.
28. J.A. Martinho Simões (2000), in *NIST Chemistry WebBook, NIST Standard Reference Database Number 69* (Mallard, W. G. and Linstrom, P. J., Ed.), National Institute of Standards and Technology, Gaithersburg, MD 20899 (http://webbook.nist.gov), pp.
29. Smith, G. P., Personal Communication, 1999.
30. Hildenbrand, D. L. and Lau, K. H., "Thermochemistry of Gaseous Manganese Oxides and Hydroxides," *J. Chem. Phys.*, **100,** 8377, 1994.
31. Rumminger, M. D., Reinelt, D., Babushok, V., and Linteris, G. T., "Numerical Study of the Inhibition of Premixed and Diffusion Flames by Iron Pentacarbonyl," *Combust. Flame*, **116,** 207, 1999.
32. Kee, R. J., Grcar, J. F., Smooke, M. D., and Miller, J. A., "A Fortran Computer Program for Modeling Steady Laminar One-dimensional Premixed Flames", Sandia National Laboratories Report, SAND85-8240, 1991.
33. Kee, R. J., Rupley, F. M., and Miller, J. A., "CHEMKIN-II: A Fortran Chemical Kinetics Package for the Analysis of Gas Phase Chemical Kinetics", Sandia National Laboratory, SAND89-8009B, 1989.
34. Kee, R. J., Dixon-Lewis, G., Warnatz, J., Coltrin, R. E., and Miller, J. A., "A Fortran Computer Package for the Evaluation of Gas-Phase, Multicomponent Transport Properties", Sandia National Laboratory, SAND86-8246, 1986.
35. Smith, G. P., Golden, D. M., Frenklach, M., Moriarty, N. W., Eiteneer, B., Goldenberg, M., Bowman, C. T., Hanson, R. K., Song, S., Gardiner, Jr. W. C., Lissianski, V. V., and Qin, Z., "GRI-Mech: An Optimized Detailed Chemical Reaction Mechanism for Methane Combustion", Gas Research Institute Topical Report, http://www.me.berkeley.edu/gri_mech, 2001.
36. Fristrom, R. M. and Sawyer, R. F., "*AGARD Conference on Aircraft Fuels, Lubricants, and Fire Safety*, *AGARD-CP 84-71*, 1971.
37. Gilman, J., Personal Communication, April, 2001.
38. Fontijn, A. and Bajaj, P. N., "*J. Phys. Chem.*, **100,** 7085, 1996.